JACS
JOURNAL OF THE AMERICAN CHEMICAL SOCIETY
Article
Cite This: J. Am. Chem. Soc. 2018, 140, 4569−4579
pubs.acs.org/JACS

Thermodynamic Hydricities of Biomimetic Organic Hydride Donors

Stefan Ilic,[†,‡] Usha Pandey Kadel,[§] Yasemin Basdogan,[⊥] John A. Keith,[⊥] and Ksenija D. Glusac*[,†,‡]

[†]Department of Chemistry, University of Illinois at Chicago, Chicago, Illinois 60607, United States
[‡]Chemical Sciences and Engineering Division, Argonne National Laboratory, Lemont, Illinois 60439, United States
[§]Department of Chemistry, Center for Photochemical Sciences, Bowling Green State University, Bowling Green, Ohio 43403, United States
[⊥]Department of Chemical and Petroleum Engineering, University of Pittsburgh, Pittsburgh, Pennsylvania 15260, United States

Supporting Information

ABSTRACT: Thermodynamic hydricities (ΔG_{H^-}) in acetonitrile and dimethyl sulfoxide have been calculated and experimentally measured for several metal-free hydride donors: NADH analogs (BNAH, CN-BNAH, Me-MNAH, HEH), methylene tetrahydromethanopterin analogs (BIMH, CAFH), acridine derivatives (Ph-AcrH, Me_2N-AcrH, T-AcrH, 4OH, 2OH, 3NH), and a triarylmethane derivative (6OH). The calculated hydricity values, obtained using density functional theory, showed a reasonably good match (within 3 kcal/mol) with the experimental values, obtained using "potential pK_a" and "hydride-transfer" methods. The hydride donor abilities of model compounds were in the 48.7−85.8 kcal/mol (acetonitrile) and 46.9−84.1 kcal/mol (DMSO) range, making them comparable to previously studied first-row transition metal hydride complexes. To evaluate the relevance of entropic contribution to the overall hydricity, Gibbs free energy differences (ΔG_{H^-}) obtained in this work were compared with the enthalpy (ΔH_{H^-}) values obtained by others. The results indicate that, even though ΔH_{H^-} values exhibit the same trends as ΔG_{H^-}, the differences between room-temperature ΔG_{H^-} and ΔH_{H^-} values range from 3 to 9 kcal/mol. This study also reports a new metal-free hydride donor, namely, an acridine-based compound 3NH, whose hydricity exceeds that of $NaBH_4$. Collectively, this work gives a perspective of use metal-free hydride catalysts in fuel-forming and other reduction processes.

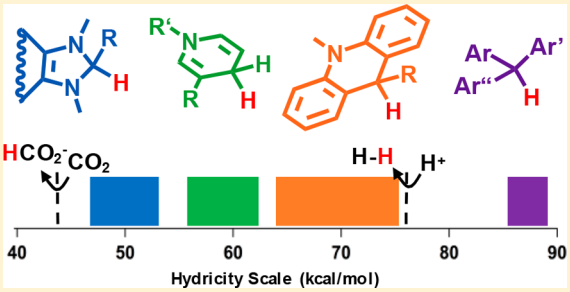

INTRODUCTION

Enzymatic redox reactions often rely on organic cofactors, such as reduced nicotine adenine dinucleotide (NADH) and flavin adenine dinucleotide ($FADH_2$), to perform hydride transfer reactions to substrates such as carbonyl compounds,[1] carbon dioxide,[2] flavins (imines),[3] and compounds containing activated C=C bonds.[4,5] The synthetic analogs of these biological "H_2-equivalents" have found applications in chemical laboratories, particularly when asymmetric transformations are desired. In the presence of a chiral cocatalyst, NADH analogs serve as regio- and enantioselective reagents for the reduction of imines to amines,[6−8] carbonyl compounds to alcohols,[8−10] and compounds with C=C bonds to the corresponding saturated analogs.[8,11,12] NADH analogs have also been applied to the fuel forming reactions. Specifically, a simple pyridinium ion has been investigated as facilitating the electrocatalytic and photoelectrocatalytic reduction of CO_2 to methanol.[13−16] While the experimental work was not reproduced by others,[16] and the mechanism of catalysis still remains unclear, the computational work indicates that the CO_2 reduction may occur by a hydride transfer from dihydropyridine, a close relative of NADH.[17−21] More recently, other nitrogen-containing organic compounds (imidazoles,[22,23] pyridazine,[24] pyridoxine,[25] mercaptopteridine,[26−28] dihydrophenanthridine,[29] and dihydroacridine[29]) have also been shown to perform CO_2 reduction reactions. Furthermore, NADH analog-based ligands coordinated with redox-active transition metal (Ru,[30] Ir[31]) or other metal ions (Al[32]) were shown to perform the photocatalytic or electrocatalytic reduction of CO_2 or water.

Thermodynamic hydricity (ΔG_{H^-}) is a useful parameter that is often used to evaluate the hydride donating ability of a molecule. It is defined as the Gibbs free energy for hydride ion release from the compound, with lower values of ΔG_{H^-} indicating better hydride donors:

$$\mathrm{R{-}H} \rightarrow \mathrm{R^+ + H^-} \qquad \Delta G_{H^-} \qquad (1)$$

This thermodynamic parameter provides useful information for the potential application of hydrides in synthetic reductions of C=C, C=N, and C=O bonds as well as in fuel-forming reductions of protons and CO_2. For this reason, the hydricities of a large number of metal-based hydrides have been extensively studied using computational and experimental methods for different solvents.[33−39] Although ΔG_{H^-} values exhibit strong solvent effects,[40−42] the majority of reported

Received: December 21, 2017
Published: March 16, 2018

DOI: 10.1021/jacs.7b13526
J. Am. Chem. Soc. 2018, 140, 4569−4579

hydricities were obtained in acetonitrile. These hydricities were found to vary in a wide 25−120 kcal/mol range. Relevant to fuel-forming reactions in acetonitrile, hydrides with ΔG_{H^-} below 76 kcal/mol are thermodynamically capable of proton reduction,[43,44] whereas ΔG_{H^-} below 44 kcal/mol is needed for the reduction of CO_2 to formate.[45] The hydricity studies on metal-based models have shown several structural factors that influence the ΔG_{H^-} values of metal hydrides: (i) The type of the metal used significantly alters the hydricities of complexes. Within the same row of the periodic table, metals with lower atomic number give rise to metal complexes with greater hydride donor ability.[46] Within the same group, metals in second and third rows are generally better hydride donors than the first-row analogues.[33,44,47,48] (ii) The structural and electronic properties of the ligand can also tune the hydricities. For example, the decrease in the ligand bite angle contributes to the lowering of ΔG_{H^-} values.[48−50] Furthermore, the presence of electron-donating substituents on the ligand decreases the hydricities of metal complexes.[44,51−53] (iii) The overall charge of the metal complex also affects the hydricities, with anionic complexes being stronger hydride donors than the corresponding neutral analogs.[54−56] (iv) Solvent drastically affects hydricities, where more polar solvents (such as water) lower ΔG_{H^-} values.[37,40,57−61] It is interesting to note that the hydricity values in different solvents do not scale linearly, making it possible for a certain reaction to be thermodynamically downhill in one solvent, while it is uphill in another.[57]

A systematic analysis of over 150 reported hydricity values for metal-based hydride donors has enabled the discovery of many elegant catalytic systems in which the critical reduction step involves a hydride transfer.[36,62] Despite being widely present in natural systems, metal-free hydrides lack proper thermodynamic evaluation. Most studies of organic compounds have focused on weaker hydride donors, such as aryl-substituted carbocations and quinones.[63−65] Among stronger organic donors, thermodynamic hydricities have been reported only for a limited number of model compounds.[56,63,64,66−68] The most hydridic donors have been found to be radical anions of organic hydride donors, such as one-electron reduced dihydroanthracenes and toluenes.[68] Even though these radical anions showed excellent hydride donating ability, very negative potentials required for their formation (<−1.5 V) and low-stability of active hydride species prevent practical application. As a general trend, the hydricities of these organic hydride donors can be lowered by increasing the stability of the cation R^+ formed upon the hydride transfer, either through aromatic stabilization or by the introduction of electron-donating groups. Due to experimental challenges associated with determination of ΔG_{H^-} values, the hydricities of metal-free donors are often reported in terms of two other parameters that can be obtained from relatively simple experimental measurements: the enthalpy change associated with the hydride release (ΔG_{H^-})[69−71] and the hydride nucleophilicity (N).[72,73] While the reported ΔG_{H^-} values allowed screening of a large number of metal-free hydrides, it is not clear whether the entropic contribution ($T\Delta G_{H^-}$) is negligible or persistent for structurally different hydride donors. Similarly, the nucleophilicity, N, is an empirical parameter that provides useful insights into the kinetics of hydride transfers from model donors, but the correlation between N values and standard kinetic parameters (such as activation free energy, $\Delta G^{‡}$) is not straightforward.

In this study, we report the calculated and experimental thermodynamic ΔG_{H^-} for model organic hydrides presented in Scheme 1. Some of the model compounds are direct analogs of the enzymatic cofactors NADH[1] (model compounds BNAH, CN-BNAH, Me-MNAH, and HEH) and methylene tetrahydromethanopterin, H_4MPT^+[74] (model compounds BIMH and CAFH). Other model compounds are derived from acridine (Ph-AcrH, Me_2N-AcrH, T-AcrH, 4OH, 2OH, 3NH) and triarylmethane (6OH) frameworks. The calculated values were determined in two solvents using density functional theory (DFT) and supported by experimental findings obtained using "potential pK_a" and hydride transfer methods. A comparison of ΔG_{H^-}values obtained here with calculated ΔH_{H^-} values indicate a degree of uncertainty associated with the evaluation of hydride strength using enthalpic ΔH_{H^-}. Specifically, the entropic contribution ($T\Delta S_{H^-}$) was found to differ significantly for structurally unrelated hydride donors. The results of our work are also discussed in terms of the structural and electronic factors that lead to good hydride donor abilities in metal-free models. Importantly, we discovered a new metal-free compound with strong hydride donating ability: an acridine-based structure, 3NH, was shown to exceed the hydride donor abilities of natural and most artificial metal-free hydride donors. Additionally, the cathodic behavior of the corresponding cation, $3N^+$, was shown to be reversible, indicating that this compound could be possibly utilized in catalysis.

Scheme 1. Structure of Organic Hydrides[a]

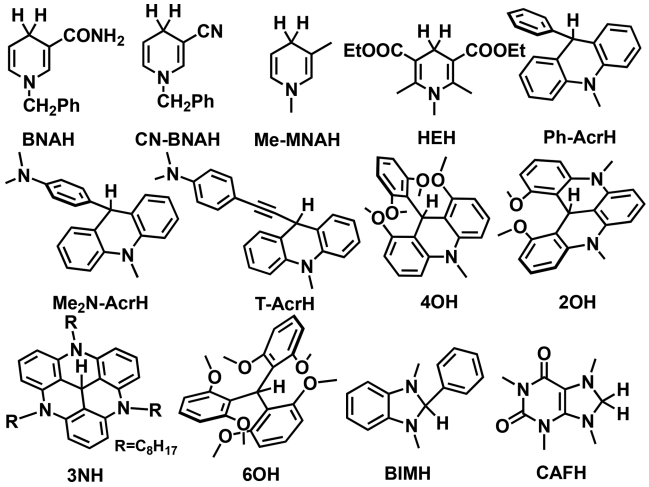

[a]NADH analogs (BNAH, CN-BNAH, Me-MNAH, HEH), methylene tetrahydromethanopterin analogs (BIMH and CAFH), acridine (Ph-AcrH, Me_2N-AcrH, T-AcrH, 4OH, 2OH, 3NH), and triarylmethane (6OH) derivatives.

COMPUTATIONAL METHODS

Hydricity Calculations. All calculations related to hydricity were performed using Gaussian 09 package[75] with the resources of the Ohio Supercomputer Center. The geometries of relevant species (R^+ and R−H) were optimized at the ωB97X-D/6-311G(d) level of theory with the conductor-like polarizable continuum model (CPCM) for solvents (acetonitrile and dimethyl sulfoxide).[76−78] The frequency calculations were performed to confirm the absence of imaginary frequencies. The output files from the frequency calculations provided the thermal corrections to free energies (ΔG^{sol}_{corr}) for R^+ and R−H. The structures optimized at the ωB97X-D/6-311G(d) level were then used to perform a single-point energy calculation at the ωB97X-D/6-311++G(2df,p)/CPCM(ACN or DMSO) level, and the electronic energies (ε^{sol}_0) of R^+ and R−H were obtained from these output files.

DOI: 10.1021/jacs.7b13526
J. Am. Chem. Soc. 2018, 140, 4569−4579

The computational method for hydricity calculation was adopted from the previously published study.[79] The hydricity of a model compound R−H is defined as the thermodynamic driving force (ΔG_{H^-}) for the following reaction:

$$R{-}H \rightarrow R^+ + H^- \qquad \Delta G_{H^-} = G_{R^+} + G_{Hyd} - G_{R-H}$$

where individual Gibbs free energies are defined as follow:

$$G_{R+} = (\varepsilon_0^{sol} + \Delta G_{corr}^{sol} + \Delta G_{0\rightarrow}^{*})_{R+}$$

$$G_{Hyd} = (\varepsilon_0^{gas} + \Delta G_{corr}^{gas} + \Delta G_{hyd}^{sol} + \Delta G_{0\rightarrow}^{*})_{Hyd}$$

$$G_{R-H} = (\varepsilon_0^{sol} + \Delta G_{corr}^{sol} + \Delta G_{0\rightarrow}^{*})_{R-H}$$

where ε_0^{sol} and ε_0^{gas} represent electronic energies in solvated and gas phases, ΔG_{corr}^{sol} and ΔG_{corr}^{gas} are thermal correction to the Gibbs free energy in solvated and gas phases, ΔG_{hyd}^{sol} is solvation free energy for the hydride anion, and $\Delta G_{0\rightarrow}^{*}$ is a standard state correction (the value is $\Delta G_{0\rightarrow}^{*}$ = +1.891 kcal/mol for all species that do not have gaseous standard state).[80,81] Electronic energies and thermal corrections to the Gibbs free energy were obtained as previously described. To derive G_{hyd}, the electronic energy (ε_0^{gas} = −331.14 kcal/mol) and the thermal correction (ΔG_{corr}^{gas} = −6.28 kcal/mol) were obtained for gas-phase using the ωB97X-D/6-31+G(d,p) level of theory. The solvation energy ΔG_{hyd}^{sol} for H^- was obtained from the thermochemical cycle connecting gas phase and solution phase one-electron reduction, as expressed in the following equation:

$$\Delta G_{hyd}^{sol} = \Delta G_{(H/H^-)}^{solv} - \Delta G_{(H/H^-)}^{gas} + \Delta G_{(H)}^{solv}$$

where $\Delta G_{(H/H^-)}^{gas}$ and $\Delta G_{(H/H^-)}^{solv}$ represent the Gibbs free energy changes for the one electron reduction of hydrogen atom in the gas phase and the solution, respectively. $\Delta G_{gas}(H/H^-)$ is the negative value of the electron affinity of hydrogen atom ($\Delta G_{gas}(H/H^-)$ = −17.39 kcal/mol[82]). $\Delta G_{(H/H^-)}^{solv}$ was obtained from the experimental one-electron potentials E_{H/H^-}^{0}: using E_{H/H^-}^{0} = −0.60 V[68] and −0.55 V[68] for acetonitrile and dimethyl sulfoxide, $\Delta G_{(H/H^-)}^{solv}$ values were estimated to be −84.88 kcal/mol and −86.04 kcal/mol for acetonitrile and dimethyl sulfoxide, respectively. $\Delta G_{(H)}^{solv}$ represents the solvation energy of hydrogen atom, and this value was computed using CPCM/6-311++G(2df,p) and found to be −0.1 kcal/mol in both solvents. Using this procedure, the computed values for G_{Hyd} were −404.8 kcal/mol and −406.0 kcal/mol for acetonitrile and dimethyl sulfoxide, respectively.

Reduction Potential Calculations. The first ($E_{R+/R^\bullet}^{\circ}$) and second ($E_{R^\bullet/R-}^{\circ}$) reduction potentials for our model compounds were derived from the calculated driving forces ($\Delta G_{R+/R^\bullet}$ and $\Delta G_{R^\bullet/R^-}$), as follows:

$$\Delta G_{R^+/R^\bullet} = (\varepsilon_0^{sol} + \Delta E_{0\rightarrow}^{*})_{R^\bullet} - (\varepsilon_0^{sol} + \Delta E_{0\rightarrow}^{*})_{R^+}$$

$$\Delta G_{R^\bullet/R^-} = (\varepsilon_0^{sol} + \Delta E_{0\rightarrow}^{*})_{R^-} - (\varepsilon_0^{sol} + \Delta E_{0\rightarrow}^{*})_{R^\bullet}$$

where electronic energies were obtained by performing single-point calculations using the B3LYP[83]-D3BJ[84] and ωB97X-D3[77] exchange correlation functionals with the Def2-TZVP[85] basis set using the SMD continuum solvation model[86] on fully optimized structures obtained using the BP86[87]-D3BJ/Def2-SVP[85] model chemistry with ORCA.[88] The entropic contributions for the reactant and product states were assumed to be similar, which resulted in their mutual cancellation. The ΔG values were then used to calculate the standard reduction potentials ($E = -\frac{\Delta G}{nF}$). The calculated values were referenced to NHE by subtracting 3.92 V[80] from computed absolute potentials.[89]

In case of second reduction potentials, accuracies of $E_{R^\bullet/R^-}^{\circ}$ reduction potentials were systematically improved compared to available experiment when a counterion (K^+) was included in both the $R^\bullet$ and R^- states, that is, using reduction potentials modeled as $R^\bullet{-}K^+$ and $R^-{-}K^+$. It seemed that adding a counterion stabilizes the anion relative to the neutral radical, and this resulted in better agreement with experiment due to error cancellation. We report our best calculated values in Table 1: first reduction potential was calculated using ωB97X-D3 calculations, while the second reduction potential is calculated with ωB97X-D3 and the counterion. The Supporting Information (Table S1) reports all calculated data.

Table 1. Calculated Standard Reduction Potentials (vs NHE) for $R^+/R^\bullet$ and $R^\bullet/R^-$, pK_a Values of RH and ΔG_{H^-} for RH in Different Solvents[a]

	DMSO				ACN
compd	$E_1(R^+/R^\bullet)$[b]	$E_2(R^\bullet/R^-)$[c]	pK_a(RH)[d]	ΔG_{H^-}[e]	ΔG_{H^-}[e]
6OH	0.08	−1.27	30.4	84.1	85.8
4OH	−0.61	−1.48	37.6	73.2	75.1
PhAcrH	−0.25	−1.17	26.1	72.8	74.9
Me_2N-AcrH	−0.30	−1.20	25.6	70.3	72.2
CN-BNAH	−0.69	−1.42	33.1	66.5	68.5
T-AcrH	−0.09	−1.02	14.9	64.7	66.6
2OH	−0.58	−1.40	27.0	61.1	62.9
HEH	−1.04	−1.50	36.0	60.6	62.5
BNAH	−0.94	−1.84	38.4	58.3	60.3
CAFH	−1.87	−1.65	45.8	51.3	53.2
Me-MNAH	−1.24	−1.63	34.1	48.7	50.3
BIMH	−1.51	−1.69	38.4	48.6	50.3
3NH	−1.07	−1.75	30.8	46.9	48.7

[a] pK_a values for RH and ΔG_{H^-} for RH in different solvents. [b] Calculated using ωB97X-D3/Def2-TZVP and the SMD continuum solvation model. [c] Calculated using ωB97X-D3/Def2-TZVP and the SMD continuum solvation model with a K^+ ion. [d] Calculated using the eq 4. [e] Calculated using ωB97X-D/6-311++G(2df,p)/CPCM (DMSO or ACN).

EXPERIMENTAL SECTION

General Methods. All chemicals were purchased from commercial suppliers and used without further purification. ^{1}H NMR spectra were recorded on a Bruker Avance III 500 MHz system. Steady-state UV/vis absorption spectra were recorded on a Varian Cary 50 UV−vis spectrophotometer. 1-Benzyl-1,4-dihydronicotinamide (BNAH) and 10-methyl-9-phenylacridinium perchlorate (Ph-Acr$^+$) was purchased from TCI America. Fluorene (FlH), triphenylmethane (Ph_3CH), diphenylyldiphenylmethane (DPE), and Super-Hydride (1 M in THF) were purchased from Sigma. NAD^+ analogs ($6O^+$,[90] $4O^+$,[90] $2O^+$,[90] $3N^+$,[91] T-Acr$^+$,[90] Me_2N-Acr$^+$,[90] BNA$^+$,[92] CN-BNA$^+$,[92] Me-MNA$^+$,[93] HE^+,[94] BIM^+,[95] and CAF^+[96]), NADH analogs (6OH,[97] 2OH,[98] Ph-AcrH,[79] CN-BNAH,[92] BIMH,[95] and CAFH[96]), indicator 9-phenylxanthene (XanH[99]) and nickel-complex ($[Ni(dmpe)_2](PF_6)_2$[100]) were synthesized according to the previously published procedures.

***N,N*-Dimethyl-4-(10-methyl-9,10-dihydroacridin-9-yl)aniline (Me_2N-AcrH).** Me_2N-Acr$^+$ (412 mg, 1 mmol) was dissolved in 5 mL of ethanol and cooled in an ice bath. Sodium borohydride (150 mg, 4 mmol, 4 equiv) was then added, and the color changed to yellow. The reaction mixture was warmed to room temperature and stirred for additional 4 h. The resulting solution was filtered, and the precipitate was washed with dichloromethane. The filtrate was extracted with dichloromethane, organic extracts were combined, and solvent was evaporated. The yellow oil was dissolved in ethanol and precipitated by addition of water. The yellow precipitate was filtered, washed with cold water, and dried under vacuum to yield 115 g (37%) of pure product. ^{1}H NMR (CD_3CN, 500 MHz): 7.30−7.23 (4H, m), 7.05 (2H, d), 7.00−6.90 (4H, m), 6.59 (2H, d), 5.13 (1H, s), 3.41 (3H, s), 2.77 (6H, s).

***N,N*-Dimethyl-4-((10-methyl-9,10-dihydroacridin-9-yl)-ethynyl)aniline (T-AcrH).** T-Acr$^+$ (120 mg, 0.27 mmol) was dissolved in 6 mL of ethanol and cooled in an ice bath. Sodium borohydride (62 mg, 1.62 mmol, 6 equiv) was added, and the reaction mixture was stirred for 2 h, which resulted in disappearance of the deep-blue color. The reaction mixture was then filtered, filtrate was discarded, and precipitate was washed with dichloromethane. Dichloromethane solution was evaporated yielding 30 mg of brownish product (33%). ^{1}H NMR (CD_3CN, 500 MHz): 7.67 (2H, d), 7.38

DOI: 10.1021/jacs.7b13526
J. Am. Chem. Soc. 2018, 140, 4569−4579

(2H, d), 7.33 (2H, t), 7.10−7.05 (4H, m), 6.73 (2H, d), 5.00 (1H, s), 3.46 (3H, s), 2.98 (6H, s).

Cyclic Voltammetry. Cyclic voltammetry was performed using a BASi epsilon potentiostat in a VC-2 voltammetry cell (Bioanalytical Systems) using platinum working electrode (1.6 mm diameter, MF-2013, Bioanalytical Systems), a nonaqueous Ag/Ag^+ reference electrode (MF-2062, Bioanalytical Systems), and a platinum wire (MW-4130, Bioanalytical Systems) as a counter electrode. The spectroscopic grade solvent DMSO and the electrolyte tetrabutylammonium perchlorate (TBAP) were purchased from Sigma-Aldrich and used as received. Fast scan rate cyclic voltammetry was performed using CHI 600 C potentiostat and platinum working electrode (CHI-107, CH instruments, 10 μm diameter). In the case of T-Acr$^+$, the second standard reduction potential was obtained by oxidation of T-Acr$^-$, which was prepared in situ from T-AcrH and potassium dimsyl.[101] Electrochemical potentials were converted to NHE by adding 0.548 V to the experimental potentials.[102]

pK_a Determination. The pK_a values of the NADH analogs were determined using the indicator anion method in DMSO.[99] Under inert atmosphere, indicators (InH) were added to a solution of potassium dimsyl ($K^+CH_3SOCH_2^-$) to generate the indicator anions (In^-). An excess of indicator solution was added to the $K^+CH_3SOCH_2^-$ to ensure the complete consumption of the base. The anion concentrations were determined using recorded absorbance and In^- extinction coefficients. Then, the colored In^- solutions were quenched by addition of small aliquots of organic hydride solutions in DMSO. The pK_a values for the organic hydrides were determined using the known indicator pK_a value and experimentally obtained equilibrium constants of the reactions between indicator anions and the hydrides. Indicators were chosen to be within 2 pK_a units from the hydrides, and indicator absorbed in visible spectrum where the other species were transparent.[99] In case of overlapping absorptions of In^- and deprotonated hydride R^- (Me_2N-Acr$^-$), the absorption of Me_2N-Acr$^-$ was subtracted using its extinction coefficient at λ_{max} for indicator In^-, as described in Supporting Information. The pK_a values of indicators used in this study are[99] triphenylmethane (Ph_3CH, pK_a = 30.6) for 4OH, diphenylyldiphenylmethane (DPE, pK_a = 29.4) for Me_2N-AcrH, 9-phenylxanthene (XanH, pK_a = 27.9) for Ph-AcrH and 6OH, and fluorene (FlH, pK_a = 22.6) for 2OH.

Hydride Transfer Studies. The hydricities of selected model compounds were obtained by determining the equilibrium constant for the hydride transfer to an appropriate acceptor with known hydride affinity. To ensure that the equilibrium constant can be reached, the reference compounds were selected so that their hydricities are within 3 kcal/mol of the hydricities of our model compounds (as estimated from DFT calculations described in the Computational Methods section). The equilibrium concentration ratios of reactants and products were obtained using ^{1}H NMR spectroscopy. The following steps were performed to ensure that equilibrium was reached: The progress of the reaction was monitored until the integration of NMR peaks stopped changing. Then, an additional amount of one of the products was added, and the reaction was monitored again until equilibrium was reached. Deuterated acetonitrile and DMSO were used as solvents. All reaction mixtures were prepared in the glovebox using dry reagents and airtight NMR tubes.

Equilibrium of BNAH and 2O$^+$. BNAH (3.8 mg, 0.018 mmol) and 2O$^+$ (8.1 mg, 0.018 mmol) were dissolved in 0.6 mL of deuterated acetonitrile or DMSO. The equilibrium constant was reached after 14 days in acetonitrile yielding K_{eq} = 9.61, whereas the equilibrium was reached after 19 days in DMSO yielding K_{eq} = 1.68. The hydricity of 2OH in acetonitrile was obtained from K_{eq} and the reported hydricity of BNAH (59 kcal/mol) as reference.[56] In the case of DMSO, the hydricity of 2OH (58.3 kcal/mol) was calculated by using the potential pK_a method, and the obtained value was used as reference to calculate the hydricity of BNAH in DMSO. The 2OH hydricity was 60 kcal/mol in acetonitrile, and the hydricity of BNAH was 57.7 kcal/mol in DMSO.

Equilibrium of BNAH and HE$^+$. BNAH (3.8 mg, 0.018 mmol) and HE$^+$ (5.5 mg, 0.018 mmol) were dissolved in 0.6 mL of deuterated acetonitrile or DMSO. In acetonitrile, the equilibrium was reached after 15 days, yielding K_{eq} = 87.52. In DMSO, the equilibrium was reached after 49 days, yielding K_{eq} = 1.53. The hydricity of HEH in acetonitrile was obtained from K_{eq} and the reported hydricity of BNAH (59 kcal/mol) as reference.[56] The hydricity of HEH in case of DMSO was obtained from K_{eq} and hydricity of BNAH (57.7 kcal/mol) as reference. The HEH hydricity was 61.5 kcal/mol in acetonitrile and 58.2 kcal/mol in DMSO.

Equilibrium of [Ni(dmpe)$_2$H]$^+$ and 3N$^+$ or BIM$^+$. [Ni(dmpe)$_2$H]$^+$ was prepared in situ by addition of 1 M Super-Hydride (20 μL, 0.020 mmol) to a solution of $[Ni(dmpe)_2](PF_6)_2$ (16.2 mg, 0.025 mmol) in 0.6 mL deuterated acetonitrile. To this solution was then added 3N$^+$ (12.7 mg, 0.025 mmol) or BIM$^+$ (8.1 mg, 0.026 mmol). The K_{eq} = 3.33 was obtained after 15 days for 3N$^+$ and K_{eq}= 0.69 was obtained for BIM$^+$ after 11 days. From these equilibrium constants and reported hydricity of [Ni(dmpe)$_2$H]$^+$ (49.9 kcal/mol),[36] we derived ΔG_{H^-}(3NH) = 49.2 kcal/mol and ΔG_{H^-}(BIMH) = 50.1 kcal/mol in acetonitrile.

RESULTS AND DISCUSSION

Calculated Hydricities. The hydricities ΔG_{H^-} of model compounds R−H (eq 1) are calculated from the absolute Gibbs energies of reactant and product states in the appropriate solvation model:

$$\Delta G_{H^-} = G_{R^+} + G_{hyd} - G_{R-H} \quad (2)$$

While the Gibbs energies of solvated R^+ and R−H species can be calculated reasonably well using the standard DFT methodology and solvation models, the calculation of absolute Gibbs free energy for the solvated hydride ion (G_{hyd}) represents a challenge. One way to overcome this drawback is to calculate the thermodynamic parameters for a hydride transfer reaction between R−H and a reference hydride acceptor (such as acridinium cation or *p*-benzoquinone) whose hydride affinity is known from the experiment.[66,103] Alternatively, the G_{hyd} value can be obtained as a fitting parameter from the experimental hydricities and calculated Gibbs energies G_{R^+} and G_{R-H}.[17,48,104,105] Unfortunately, G_{hyd} values derived from these studies are not consistent (for example, G_{hyd} values in acetonitrile were reported to be −400.7 kcal/mol,[48] − 404.7 kcal/mol,[105] and −412.7 kcal/mol[104]).

In collaboration with the Krylov group at the University of Southern California, we previously calculated the hydricity of an acridine-based hydride donor, and the obtained value was in excellent agreement with the experimental hydricity.[79] In our approach, the absolute Gibbs energy G_{hyd} was obtained as the sum of the gas-phase energy G^{gas}_{hyd} and the solvent contribution ΔG^{sol}_{hyd}:

$$G_{hyd} = G^{gas}_{hyd} + \Delta G^{sol}_{hyd} \quad (3)$$

The gas phase energy, G^{gas}_{hyd}, was calculated using DFT, while the solvation energy, ΔG^{sol}_{hyd}, was derived from the experimental one-electron reduction potential of hydrogen atom in a solvent of interest[65] and the calculated gas-phase electron affinity of a H atom (as detailed in the Computational Methods section). The G_{hyd} values obtained in this way are −404.8 kcal/mol (in ACN) and −406.0 kcal/mol (in DMSO). In the current manuscript, this computational methodology was used to calculate the hydricities of our model hydrides in two solvents (ACN and DMSO, Table 1).

The calculations were also used to estimate the standard reduction potentials and pK_a values of relevant species (Table 1). While $E_1(R^+/R^\bullet)$ values acquired using sole electronic energies showed a reasonable match with experimental values (Table S1, Supporting Information), the $E_2(R^\bullet/R^-)$ values

DOI: 10.1021/jacs.7b13526
J. Am. Chem. Soc. 2018, 140, 4569−4579

using standard procedures did not match experiment well (mean unsigned error = 0.17 V). Since our original calculated E_2 values were consistently too negative compared to experiment, we speculated this was because the calculated free energies of R^- states were systematically too unstable regardless of different exchange correlation functionals, continuum solvation methods, and basis set sizes. As a simple correction and following previous work,[106] we added a positively charged counterion, K^+, into the calculations on the R^- and $R^\bullet$ states, and the resulting E_2 values agreed with available experimental data much better (mean unsigned error = 0.08 V). Adding an analogous counterion, Cl^-, to the states needed for the E_1 calculations did not improve the agreement of calculated versus experiment. The obtained calculated reduction potentials are then used to estimate the pK_a values for the model hydride donors (eq 4). However, the calculated pK_a values (Table 1) are not very accurate. The trends of reduction potentials and pK_a values will be discussed in a later section when experimental values are introduced.

$$pK_a^{RH} = \frac{\Delta G_{H^-} - 23.06(E^0_{R^+/R^\bullet} + E^0_{R^\bullet/R^-}) - \Delta G^{H^+/H^-}_{solvent}}{1.364} \quad (4)$$

Experimental Hydricities. Two experimental approaches were used to determine the hydricities of model compounds: the "potential pK_a" and "hydride transfer" methods.[36] The potential pK_a method uses the relevant standard reduction potentials and pK_a values to determine the hydricity of a model compound, as follows:

$$R^+ + e^- \rightarrow R^\bullet \qquad \Delta G_{ET1} = -23.06E^0_{R^+/R^\bullet}$$

$$R^\bullet + e^- \rightarrow R^- \qquad \Delta G_{ET2} = -23.06E^0_{R^\bullet/R^-}$$

$$R^- + H^+ \rightarrow RH \qquad \Delta G_{PT} = -1.364pK_a^{RH}$$

$$H^+ + 2e^- \rightarrow H^-$$

$$\Delta G^{H^+/H^-}_{DMSO} = 69.9 \text{ kcal/mol}; \ \Delta G^{H^+/H^-}_{ACN} = 54.7 \text{ kcal/mol}$$

$$RH \rightarrow R^+ + H^-$$

$$\Delta G_{H-} = \Delta G_{ET1} + \Delta G_{ET2} + \Delta G_{PT} + \Delta G^{H^+/H^-}_{DMSO/ACN}$$

where ΔG_{ET1} and ΔG_{ET2} represent Gibbs free energy changes for first and second electron reduction of NAD^+ analogs, calculated using their reduction potentials ($E^0_{R^+/R^\bullet}$ and $E^0_{R^\bullet/R^-}$); ΔG_{PT} represent a Gibbs free energy change for protonation of R^-, calculated using the pK_a values of NADH analogs (pK_a^{RH}); $\Delta G^{H^+/H^-}_{DMSO}$ and $\Delta G^{H^+/H^-}_{ACN}$ represent Gibbs free energy changes for two electron reduction of the proton in dimethyl sulfoxide and acetonitrile, respectively, using the derived potentials for proton reduction in these solvents;[68] ΔG_{H^-} represents hydricity of the studied NADH analog.

The hydride transfer method involves the determination of the equilibrium constant (K_{HT}) for a hydride transfer from a model hydride R–H and a reference hydride acceptor (A^+) with known affinity, as follows:

$$RH + A^+ \rightleftharpoons R^+ + AH \qquad \Delta G_{HT} = -RT \ln K_{HT}$$

$$AH \rightarrow A^+ + H^- \qquad \Delta G_{H-}(AH)$$

$$RH \rightarrow R^+ + H^-$$

$$\Delta G_{H-}(RH) = \Delta G_{H-}(AH) + \Delta G_{HT}$$

where ΔG_{HT} represents a Gibbs free energy change for the hydride transfer between examined and referent hydrides, calculated from experimentally obtained equilibrium constant for the hydride transfer, K_{HT}; $\Delta G_{H^-}(AH)$ and $\Delta G_{H^-}(RH)$ represent hydricities of the reference and examined hydrides.

Both of these approaches have limitations, which necessitated the use of potential pK_a method for those model compounds that exhibited measurable reduction potentials and pK_a values in DMSO. On the other hand, the hydride transfer method was used for the model compounds that reached the equilibrium point when reacted with the reference hydride acceptor.

Potential pK_a Method. While this experimental approach is relatively simple, it is limited to the model compounds whose reduction potentials, $E^0_{R^+/R^\bullet}$ and $E^0_{R^\bullet/R^-}$, are within the electrochemical window of the electrolyte solution (approximately −1.9 V vs NHE for DMSO using TBAP as electrolyte and platinum working electrode). Furthermore, the pK_a values of hydride donors R–H can be experimentally determined only if R–H is more acidic than the solvent (for DMSO, pK_a = 35, which limits the pK_a determination for compounds with pK_a values lower than 32).[107] The calculated pK_a values in Table 1 indicate that the acidity of CN-BNAH, Me-MNAH, HEH, 4OH, BNAH, BIMH, and CAFH are higher than that of the DMSO limit, indicating that their hydricities are not likely to be determined using the potential pK_a method. However, this argument should be taken loosely due to the low accuracy of calculated pK_a values. Similarly, the reduction potentials $E^0_{R^+/R^\bullet}$ and $E^0_{R^\bullet/R^-}$ need to be less negative than the cathodic electrochemical window of the solvent (approximately −1.9 V vs NHE for DMSO using TBAP as electrolyte and platinum working electrode).

Standard reduction potentials were obtained using cyclic voltammetry (Figure 1). At low sweep rates, the first reduction step of $6O^+$ and most acridine-based models (Ph-Acr^+, Me_2N-Acr^+, $4O^+$, $2O^+$, and $3N^+$) exhibited reversible electrochemical behavior, indicating good chemical stability of the correspond-

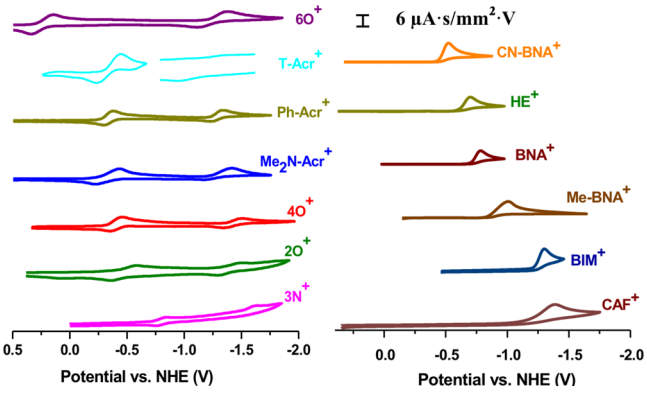

Figure 1. Cyclic voltammograms of model compound (cations) in the cathodic range: Pt working electrode, Pt counter electrode, and nonaqueous $Ag/AgNO_3$ reference electrode. Sweep rate, 0.1 V/s ($3N^+$, CN-BNA^+, HE^+, BNA^+, Me-$MBNA^+$, BIM^+, and CAF^+), 25 V/s ($6O^+$, T-Acr^-, Me_2N-Acr^+, $2O^+$), 2 kV/s (T-Acr^+), 100 V/s (Ph-Acr^+, $4O^+$); electrolyte, 0.1 M TBAP in DMSO. The second reduction peak of T-Acr^+ was obtained from the oxidation of T-Acr^-, which was formed in situ by the deprotonation of T-AcrH in the presence of dimsyl anion (pK_a = 35).[107]

DOI: 10.1021/jacs.7b13526
J. Am. Chem. Soc. 2018, 140, 4569–4579

ing radicals. On the other hand, the first reduction potentials of pyridinium (CN-BNA$^+$, HE$^+$, BNA$^+$ and Me-MNA$^+$) and imidazolium (BIM$^+$ and CAF$^+$) models appear at more negative potentials and are chemically irreversible, possibly due to radical dimerization.[108−111] The stability of pyridine-based radicals can be increased by the introduction of substituents in the 4-position.[110] The lower reactivity of acridine-based radicals over the pyridine-based structures is likely due to higher delocalization of the unpaired spin in the acridine-based radicals.[109] The reduction of T-Acr$^+$ becomes chemically reversible only at high scan rates (2 kV/s, Figure 1), despite the fact that the compound is acridine-based. The origin of the chemical irreversibility has not been explored further, but it is interesting to note that the reduction of the neutral acridine-based analog to form the radical anion is chemically reversible even at 100 mV/s.[112] The chemical instability of imidazolium radicals has been previously attributed to either their dimerization[111] or the loss of H atom and formation of carbene analogs.[111,113−115] While the one-electron reduced CAF$^+$ can form carbene analogs by a loss of a hydrogen atom from the carbon located between two N-centers, it is not clear whether BIM$^+$ can undergo similar chemistry by a loss of a phenyl radical. The chemical reversibility for the one-electron reduction of pyridinium and imidazolium models could not be achieved (scan rates up to 10 kV/s were investigated), which prevented us from obtaining the standard reduction potentials for these processes.

The second reduction peak was obtained only for NAD$^+$ analogs whose first reduction peaks were reversible (6O$^+$, Ph-Acr$^+$, Me$_2$N-Acr$^+$, 4O$^+$, 2O$^+$, and 3N$^+$). At low scan rates (100 mV/s), second reduction peaks were irreversible, likely due to the protonation of the generated anion to form NADH analogs.[116] Consistent with this assignment is the fact that the reactivity of NAD$^-$ anions (reversibility of the second reduction peak) correlates well with pK_a values of the corresponding R−H analogs. For example, the second reduction peak of 6O$^+$ becomes reversible at relatively low scan rates (25 V/s), which is consistent with relatively low basicity of 6O$^-$ anion (the pK_a of 6OH is 26.9, see text below). On the other hand, the reversibility for 4O$^+$ requires the scan rates of 100 V/s and the pK_a of 4OH is 30.3 (Table 2). In the case of T-Acr$^+$, the

Table 2. Experimentally Obtained $E^0_{R^+/R^\bullet}$ and $E^0_{R^\bullet/R^-}$ (V vs NHE), pK_a^{RH} of NADH model, and ΔG_{H^-} (kcal/mol) Values Derived Using Potential pK_a Method in Dimethyl Sulfoxide

compd	$E^0_{R^+/R^\bullet}$	$E^0_{R^\bullet/R^-}$	pK_a^{RH}	ΔG_{H^-}
6OH	+0.24	−1.24	26.9	83.5 ± 3
4OH	−0.38	−1.41	30.4	70.2 ± 3
PhAcrH	−0.29	−1.23	28.3	73.5 ± 2
Me$_2$N-AcrH	−0.30	−1.42	29.2	70.1 ± 2
T-AcrH	−0.22	−1.07	*a*	*a*
2OH	−0.50	−1.39	23.4	58.2 ± 2
3NH	−0.80	−1.62	*a*	*a*

[a]Not available.

standard reduction potential for this process was obtained by electrochemical oxidation of T-Acr$^-$ anion, formed by the deprotonation of T-AcrH (Figure 1). A similar approach was attempted on the compounds that lacked second reduction peaks, but the experiment was not successful because the dimsyl base was not a sufficiently strong base to deprotonate hydrides.

The experimental pK_a values for selected hydrides in DMSO were obtained using the spectrophotometric method developed by Bordwell.[99] The indicators with known pK_a values were deprotonated using the dimsyl anion and then reacted with model NADH analogs. The equilibrium constant for the proton transfer between the NADH analog and indicator anion was determined by monitoring the absorption of indicator anion at a selected wavelength (see Figure S2, for example). The accuracy of this method is high (0.05 pK_a units) if the acidities of indicator and NADH analog are within 2 pK_a units to ensure that the equilibrium is reached.[99] For this reason, more than one indicator was used to determine the pK_a values of model NADH analogs (Figure 2). In case of Me$_2$N-AcrH, the

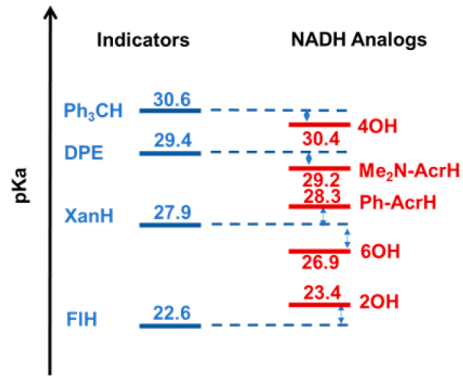

Figure 2. Indicators and their pK_a values (left) used to determine the pK_a values of NADH analogs (right): triphenylmethane (Ph$_3$CH), diphenylyldiphenylmethane (DPE), 9-phenylxanthene (XanH) and fluorene (FlH).[107]

absorption of deprotonated NADH analog overlapped with the absorption of indicator anion. In this instance, the absorption contribution due to the deprotonated NADH analog was accounted for, as described in the Supporting Information. Deprotonation of T-AcrH led to unstable products, which prevented us from determining the pK_a value of T-AcrH. Also, the same methods could not be applied for the acetonitrile, since the NADH analogs are even weaker acids in this solvent. The obtained pK_a values in DMSO were used, along with the standard reduction potentials, to determine the hydricities of model NADH analogs, and the values are reported in Table 2.

Hydride Transfer Method. The hydricities of almost one-half of the model NADH analogs presented in Scheme 1 could not be obtained using the potential pK_a method (either due to the irreversible reduction behavior of NAD$^+$ analogs or due to the high pK_a values of the corresponding R−H). The hydricities of these model compounds were obtained using the hydride-transfer method, which was previously used by Dubois to obtain the hydricities of NADH analogs (BNAH and CN-BNAH) in acetonitrile, using the metal-based hydride donors as references.[56] This study showed that the accurate equilibrium constants can be obtained if the hydricities of two relevant hydrides differ by less than 3 kcal/mol. In our study, NMR spectroscopy was used to determine the hydricities of model NADH analogs in two solvents, acetonitrile and dimethyl sulfoxide, and the results are listed in Table 3. As an example, the NMR spectra for the reaction between BNAH (reference hydride), and 2O$^+$ in acetonitrile is presented in Figure S3, Supporting Information. Unfortunately, the hydride transfer method could not be applied to all model compounds, due to

DOI: 10.1021/jacs.7b13526
J. Am. Chem. Soc. 2018, 140, 4569−4579

Table 3. Hydricities (ΔG_{H^-}, kcal/mol) of Selected Model NADH Analogs Obtained Using Hydride-Transfer Method in Dimethylsulfoxide and Acetonitrile

compound	reference hydride (ΔG_{H^-})	ΔG_{H^-}
	DMSO	
BNAH	2OH (58.2)	57.5 ± 2
HEH	BNAH (57.5)	58 ± 2
	2OH (58.2)	57.9 ± 2
	ACN	
BNAH	CpRe(NO)(CO)(CHO) (55)[56]	59 ± 2[56]
2OH	BNAH (59)[56]	60.3 ± 2
HEH	BNAH (59)[56]	61.5 ± 2
	CNBNAH (63)[56]	61 ± 2
CN-BNAH	BNAH (59)[56]	63 ± 2[56]
BIMH	$[Ni(dmpe)_2H]^+$ (49.9)[36]	50.1 ± 2
3NH	$[Ni(dmpe)_2H]^+$ (49.9)[36]	49.2 ± 2

the occurrence of unwanted side reactions. Experimental hydricity values obtained by potential pK_a and hydride transfer methods are further validated by cross-referencing among studied model compounds (see Supporting Information for more details).

Theory versus Experiment. The experimental hydricities obtained using potential pK_a and hydride transfer methods showed a good match with the calculated values (Figure 3).

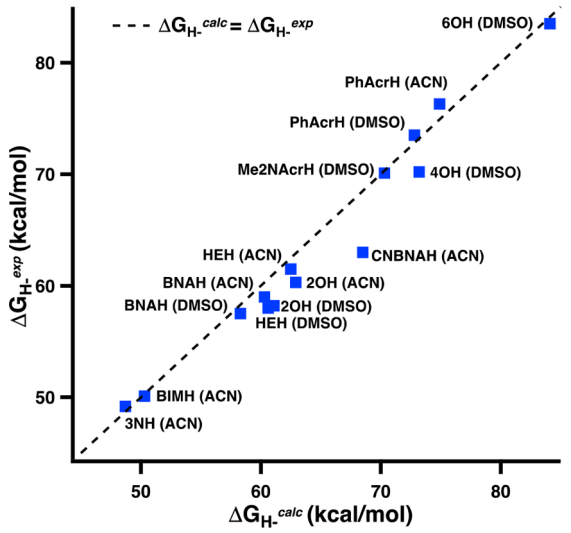

Figure 3. Comparison between the calculated and experimental hydricities for the NADH analogs. The value for PhAcrH was obtained from our ref 79, while the values for BNAH and CN-BNAH were obtained from ref 56.

The calculated values are frequently higher than the experimental hydricities by up to 3 kcal/mol, likely due in part to the uncertainties associated with the treatment of the hydride ion solvation in calculations. A similar match between experiment and theory has been reported previously for metal-based hydrides.[33,48] Our finding that computationally inexpensive methods reproduce the experimental hydricities is quite encouraging, particularly in light of technical difficulties associated with determination of experimental values.

Entropic Contributions. The experimental determination of ΔG_{H^-} values can be quite challenging, as shown in the previous section. On the other hand, the enthalpy for hydride transfer, ΔH_{H^-}, is readily obtained by a simple calorimetry method, and this method has been used to screen a large number of metal-free hydride donors. While the enthalpy approach is quite useful, the use of ΔH_{H^-} to describe hydride donor ability is justified only when entropic contributions are negligible. To evaluate the entropic contribution, we compared the ΔG_{H^-} and ΔH_{H^-} values obtained by us and others[56,69,71,103,117−119] in Figure 4. The data clearly show that the entropic contribution for metal-free hydrides cannot be ignored, with $T\Delta S_{H^-}$ values ranging from 3.4 to 12.1 kcal/mol. Thus, the assumption that the entropic contribution can be neglected introduces, on average, a 10% error to the measurement.

A more accurate approach is to assume that the entropic contribution is constant across a series of structurally related hydride donors. This assumption was found to be valid for tungsten hydride complexes ($T\Delta S_{H^-}$ = 3.2 kcal/mol).[54] While this assumption drastically reduces the error, the ΔS_{H^-} values are not always constant across series. NADH analogs exhibit $T\Delta S_{H^-}$ values in a narrow range (4.4−5.2 kcal/mol), whereas the acridine derivatives were found to have values in much wider range (3.4−6.5 kcal/mol). Thus, the enthalpic hydricity ΔH_{H^-} can be used to predict trends within the structurally related hydride donors, but it fails to give precise driving forces for hydride transfer reactions with hydrides of different groups.

Structure−Property Relationship. Based on the calculated and experimental data presented here, several interesting points can be raised regarding the structural factors that control hydricities of organic donors. In general, the hydride donor ability of R−H derivatives improves with an increase in the stabilization of the forming cation, R^+. Consequently, triarylmethane derivative showed the poorest hydride donor ability, where the R^+ stabilization is achieved solely through non-aromatic delocalization. The positive charge in R^+ can be stabilized through the inductive effect of electron-donating substituents, as can be observed for the NADH analogs, where the replacement of electron-withdrawing amide (BNAH, ΔG_{H^-} = 59 kcal/mol) or cyano (CN-BNAH, ΔG_{H^-} = 63 kcal/mol) groups with the electron-donating methyl group (Me-MNAH, ΔG_{H^-} = 50 kcal/mol) has a strong effect on hydricity. In another example, the hydricity of Me_2N-AcrH (ΔG_{H^-} = 70.1 kcal/mol) is lower relative to the derivative without donating group (PhAcrH, ΔG_{H^-} = 73.5 kcal/mol).

An interesting class of hydride donors are imidazoles (BIMH and CAFH), which have shown low hydricities (calculated ACN values in the 50−53 kcal/mol range) in accordance from previously reported ΔH_{H^-}.[69] The high hydride donor ability of imidazole derivatives has been previously credited to the specific conformation and an anomeric effect,[120] where neighboring nitrogen centers destabilize the C−H bond in R−H by donating their lone pairs to its antibonding orbital. It is interesting to note that imidazole-based hydride donors have been identified in a relatively new class of hydrogenases, namely, 5,10-methenyltetrahydromethanopterin (Hmd) hydrogenase.[121] In this enzyme, the imidazole-based hydride donor drives H_2 heterolysis reaction, activated by the presence of Fe-containing cofactor. Since the synthetic procedures for these derivatives are relatively straightforward, it is likely that new imidazole-based hydride donors will be reported in the near future.

Strikingly, the strongest hydride donor among the studied compounds was found to be an acridine derivative, 3NH (calculated ΔG_{H^-} = 49 kcal/mol in ACN). This finding is surprising, considering that the increase in the number of fused

DOI: 10.1021/jacs.7b13526
J. Am. Chem. Soc. 2018, 140, 4569−4579

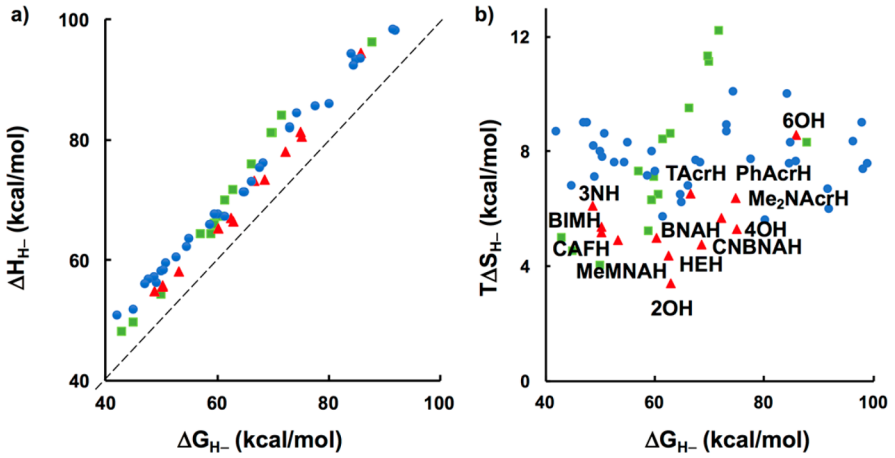

Figure 4. (a) Comparison between ΔH_{H^-} and ΔG_{H^-} for organic and other metal-free hydride donors in acetonitrile. (b) Comparison between $T\Delta S_{H^-}$ and ΔG_{H^-} for organic hydride donors. Hydrides are represented as follows: calculated values for hydrides studied here (red triangles), calculated values by others (blue circles), and experimental values obtained elsewhere (green squares). A complete list of metal-free hydrides can be found in Figure S5, Supporting Information.

aromatic rings leads to the lowering of aromatic stabilization in the corresponding R^+ cation. For example, dihydropyridines are better hydride donors than dihydroacridines, because of the higher aromatic character of pyridinium cation.[103] In the case of $3N^+$, the aromatic moiety is stabilized through the positive charge delocalization via the conjugation with the remainder of the molecule. In addition, a significant structural strain present in the rigid 3NH further facilitates the loss of a hydride ion, resulting in a highly planar system. The effects of extended charge delocalization and planarization prevails in 4OH < 2OH < 3NH series where hydricity in ACN declines from 75 to 49 kcal/mol.

It is interesting to note that acridine-based hydrides studied here (3NH and 2OH) have comparable hydricity values to other known reducing reagent, such as sodium borohydride ($NaBH_4$, calculated ΔG_{H^-} = 50 kcal/mol[117] in ACN) and Hantzsch ester (ΔG_{H^-} = 59 kcal/mol[117] in ACN). Despite being commonly utilized in organic synthesis, these hydrides are used in stoichiometric rather catalytic amounts, due to challenges associated with their regeneration.[122] The electrochemical recovery of NADH analogs is complicated by the chemical side reactions involving one-electron reduced species (such as radical dimerization).[108,109] Unlike NADH analogs, $3N^+$ and $2O^+$ exhibit electrochemically and chemically reversible reduction potentials (Figure 1), suggesting that 3NH and 2OH can be electrochemically recovered and could possibly serve as renewable hydride donors.

Overall, the hydride donor abilities were improved slightly going from acetonitrile to dimethyl sulfoxide (by ~2 kcal/mol), which was also predicted by calculations. Such a trend can be explained by the small differences in their dielectric constants (ε(DMSO) = 47 versus ε(ACN) = 38), which results in slightly better solvation of formed charged species (R^+ and H^-). A similar solvent trend has been observed for the Ni-based hydride,[40] whose hydricities were obtained in acetonitrile (ΔG_{H^-} = 57.4 kcal/mol), dimethyl sulfoxide (ΔG_{H^-} = 55.5 kcal/mol), and water (ΔG_{H^-} = 30.0 kcal/mol).

Comparison with Metal-Based Analogs. Transition metal hydrides have been identified as important intermediates in a variety of catalytic fuel-forming and other redox reactions in ground and excited state.[35,45,123−127] On the other hand, the metal-free hydrides have not been widely used for this purpose, despite the abundance of enzymatic catalysis by NADH, $FADH_2$, and other metal-free hydrides.[1−5,121] Thus, it is interesting to compare the thermodynamic hydricities of our model compounds with those reported for metal-based hydrides. In general, the hydricities of metal-based hydrides span a wide range of values (reported acetonitrile hydricities are in the 26−120 kcal/mol range[34,36]). The metal-free hydrides of Scheme 1 exhibit values that are somewhat higher, with the calculated values in the 49−86 kcal/mol range, and seem to have hydricities similar to the first raw transition metal hydrides, such as Co-, Ni-, and Fe-based compounds (acetonitrile hydricities are in the 32−73 kcal/mol range[36]). Thus, both types of compounds are sufficiently strong hydride donors for the relevant fuel forming reactions. For example, the hydride affinity of protons in acetonitrile is approximately −76.6 kcal/mol,[43] indicating that most metal-free hydride donors in Scheme 1 are thermodynamically capable of driving the hydrogen evolution reaction.

Why are then metal-free hydride donors not used in fuel-forming reactions as often as their metal-based analogs? One possible explanation might be related to the differences in the activation barriers associated with the relevant hydride transfer processes (our future studies will investigate the kinetic effect in more detail). Another reason for lower use of metal-free hydride catalysts might be related to the closure of catalytic cycle, which involves the two-electron, proton-coupled reduction of R^+ to recover the active R−H hydride form. To exemplify this point, Figure 5 presents an energy diagram for two hydride donors of similar hydricities: a metal-based $[Ni(P^{Ph}{}_2N^{Ph})_2H]^+$ complex, whose hydricity in acetonitrile is ΔG_{H^-} = 59.3 kcal/mol,[128] and 2OH, whose hydricity is ΔG_{H^-} = 60.3 kcal/mol. The first reduction potentials of the corresponding precursors, $E(M^{2+}/M^+)$ and $E(R^+/R^\bullet)$, are relatively similar and affordably small (around −0.5 V vs NHE). Previous studies of metal-based compounds have shown that $E(M^{2+}/M^+)$ shifts to more negative values as the hydride donor ability of the corresponding donor increases.[36,52,129−131] Our metal-free analogs scale in the same way, as exemplified by the similarities in the first reduction peaks for M^{2+}/M^+ and $R^+/R^\bullet$. However, a striking difference was observed in the values for the second reduction potentials, $E(M^+/M^0)$ and $E(R^\bullet/R^-)$: while the metal-based compound undergoes the second

DOI: 10.1021/jacs.7b13526
J. Am. Chem. Soc. 2018, 140, 4569−4579

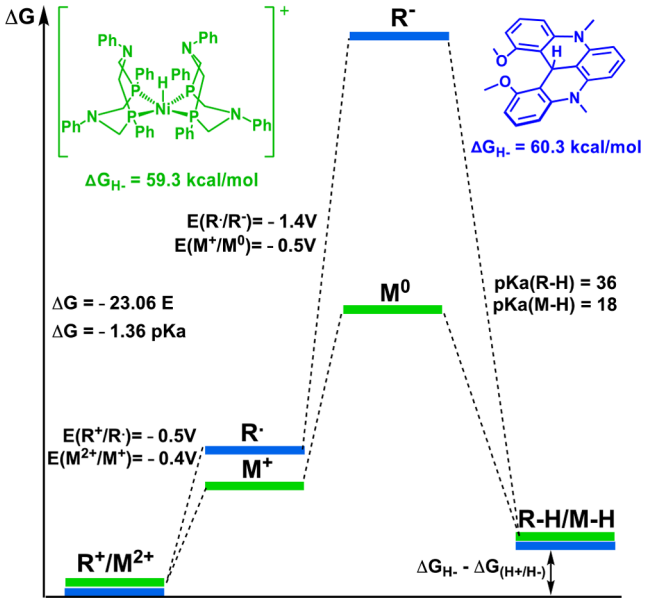

Figure 5. Comparison of energy diagram profiles for the regeneration of active hydride forms of metal-based ($[Ni(P^{Ph}_2N^{Ph})_2H]^+$)[128] and metal-free (2OH) hydride donors.

reduction at a relatively low potential (−0.5 V vs NHE), the metal-free model compound requires a significantly more negative potential (−1.4 V vs NHE) to inject the second electron.

Such a large energy requirement for the second reduction step prohibits the application of metal-free hydride donors in catalysis. Several approaches can be used to lower the standard reduction potentials in metal-free systems. One involves the coupling of the first electron transfer step with a proton transfer to generate $RH^{\bullet+}$, which will then be reduced at a less negative potential. Such proton-coupled reduction has been selected by nature as a way to regenerate NADH. Specifically, NAD^+ reduction is mediated by $FADH_2$, which is formed from FAD^+ through two proton-coupled reductions.[132] Another interesting approach toward the lowering of reduction potentials has recently been reported by Berben and co-workers, who utilized the coordination with Al ions to lower the reduction potentials of imine-based ligands.[32] Finally, model compounds that exhibit small or even inverted differences in reduction potentials can be utilized to facilitate the regeneration of metal-free hydrides.[133] For example, it was shown for some organic compounds that the structural changes that accompany the first electron reduction can result in the lowering of their LUMO orbital energies and associated second reduction potentials.[134] We observe similar effects in the case of BIM^+, which exhibits the smallest energy difference between the calculated $E(R^+/R^{\bullet})$ and $E(R^{\bullet}/R^-)$ potentials (Table 1), likely brought about by the rotation of the phenyl ring upon one electron reduction (Figure S4, Supporting Information).

CONCLUSIONS

Despite their importance in enzymatic redox reactions, metal-free hydride donors are not widely used as catalysts for fuel-forming and other reduction processes. To explore their applicability in catalysis, we investigated hydricities of several model compounds that are direct analogs of the enzymatic cofactors NADH and methylene tetrahydromethanopterin, as well as the synthetic hydrides derived from acridine and triarylmethane frameworks. The hydride donor ability for the model compounds reported here were found to be similar to metal-based hydrides and dependent on structural motifs, such as size of conjugated molecular framework, aromaticity, and presence of electron-donating groups. Unlike the metal-based equivalents, the metal-free hydrides exhibited high values for their second reduction potentials, prohibiting the catalyst recovery. Future design of these hydride donors will be focused on lowering the reduction potentials and enabling facile hydride-form regeneration.

ASSOCIATED CONTENT

Supporting Information

The Supporting Information is available free of charge on the ACS Publications website at DOI: 10.1021/jacs.7b13526.

^{1}H NMR spectra, coordinates for optimized structures, calculated reduction potentials, pK_a-determination experiment and hydride-transfer method, and enthalpic contributions (PDF)

AUTHOR INFORMATION

Corresponding Author

*glusac@uic.edu

ORCID

John A. Keith: 0000-0002-6583-6322

Ksenija D. Glusac: 0000-0002-2734-057X

Notes

The authors declare no competing financial interest.

ACKNOWLEDGMENTS

K.D.G. thanks ACS PRF (54436-ND4) for financial support and Ohio Supercomputer Center (PCS0201-5) for computational support. J.A.K. acknowledges support from the R.K. Mellon Foundation, ACS PRF (55595-DNI4), and the National Science Foundation (CBET-1653392).

REFERENCES

(1) Hummel, W. *Trends Biotechnol.* **1999**, *17* (12), 487−492.

(2) Reda, T.; Plugge, C. M.; Abram, N. J.; Hirst, J. *Proc. Natl. Acad. Sci. U. S. A.* **2008**, *105* (31), 10654−10658.

(3) Schrittwieser, J. H.; Velikogne, S.; Kroutil, W. *Adv. Synth. Catal.* **2015**, *357* (8), 1655−1685.

(4) Stueckler, C.; Hall, M.; Ehammer, H.; Pointner, E.; Kroutil, W.; Macheroux, P.; Faber, K. *Org. Lett.* **2007**, *9* (26), 5409−5411.

(5) Stuermer, R.; Hauer, B.; Hall, M.; Faber, K. *Curr. Opin. Chem. Biol.* **2007**, *11* (2), 203−213.

(6) Rueping, M.; Sugiono, E.; Azap, C.; Theissmann, T.; Bolte, M. *Org. Lett.* **2005**, *7* (17), 3781−3783.

(7) Ouellet, S. G.; Walji, A. M.; Macmillan, D. W. *Acc. Chem. Res.* **2007**, *40* (12), 1327−1339.

(8) Zheng, C.; You, S.-L. *Chem. Soc. Rev.* **2012**, *41* (6), 2498−2518.

(9) Rueping, M.; Antonchick, A. P.; Theissmann, T. *Angew. Chem., Int. Ed.* **2006**, *45* (22), 3683−3686.

(10) Yang, J. W.; List, B. *Org. Lett.* **2006**, *8* (24), 5653−5655.

(11) Yang, J. W.; Hechavarria Fonseca, M. T.; List, B. *Angew. Chem., Int. Ed.* **2004**, *43* (48), 6660−6662.

(12) Ouellet, S. G.; Tuttle, J. B.; MacMillan, D. W. *J. Am. Chem. Soc.* **2005**, *127* (1), 32−33.

(13) Seshadri, G.; Lin, C.; Bocarsly, A. B. *J. Electroanal. Chem.* **1994**, *372* (1), 145−150.

(14) Barton, E. E.; Rampulla, D. M.; Bocarsly, A. B. *J. Am. Chem. Soc.* **2008**, *130* (20), 6342−6344.

DOI: 10.1021/jacs.7b13526
J. Am. Chem. Soc. 2018, 140, 4569−4579

(15) Polyansky, D.; Cabelli, D.; Muckerman, J. T.; Fujita, E.; Koizumi, T. a.; Fukushima, T.; Wada, T.; Tanaka, K. *Angew. Chem., Int. Ed.* **2007**, *46* (22), 4169−4172.
(16) Costentin, C.; Canales, J. C.; Haddou, B.; Savéant, J.-M. *J. Am. Chem. Soc.* **2013**, *135* (47), 17671−17674.
(17) Lim, C.-H.; Holder, A. M.; Hynes, J. T.; Musgrave, C. B. *J. Am. Chem. Soc.* **2014**, *136* (45), 16081−16095.
(18) Lim, C.-H.; Holder, A. M.; Hynes, J. T.; Musgrave, C. B. *J. Phys. Chem. Lett.* **2015**, *6* (24), 5078−5092.
(19) Keith, J. A.; Carter, E. A. *Chem. Sci.* **2013**, *4* (4), 1490−1496.
(20) Keith, J. A.; Carter, E. A. *J. Phys. Chem. Lett.* **2013**, *4* (23), 4058−4063.
(21) Lessio, M.; Senftle, T. P.; Carter, E. A. *ACS Energy Lett.* **2016**, *1* (2), 464−468.
(22) Liao, K.; Askerka, M.; Zeitler, E. L.; Bocarsly, A. B.; Batista, V. S. *Top. Catal.* **2015**, *58* (1), 23−29.
(23) Bocarsly, A. B.; Gibson, Q. D.; Morris, A. J.; L'Esperance, R. P.; Detweiler, Z. M.; Lakkaraju, P. S.; Zeitler, E. L.; Shaw, T. W. *ACS Catal.* **2012**, *2* (8), 1684−1692.
(24) Portenkirchner, E.; Enengl, C.; Enengl, S.; Hinterberger, G.; Schlager, S.; Apaydin, D.; Neugebauer, H.; Knör, G.; Sariciftci, N. S. *ChemElectroChem* **2014**, *1* (9), 1543−1548.
(25) Lee, J. H.; Lauw, S. J.; Webster, R. D. *Electrochem. Commun.* **2016**, *64*, 69−73.
(26) Xiang, D.; Magana, D.; Dyer, R. B. *J. Am. Chem. Soc.* **2014**, *136* (40), 14007−14010.
(27) Saveant, J.-M.; Tard, C. d. *J. Am. Chem. Soc.* **2016**, *138* (3), 1017−1021.
(28) Lim, C.-H.; Holder, A. M.; Hynes, J. T.; Musgrave, C. B. *J. Phys. Chem. B* **2017**, *121* (16), 4158−4167.
(29) Giesbrecht, P. K.; Herbert, D. E. *ACS Energy Lett.* **2017**, *2* (3), 549−555.
(30) Kobayashi, K.; Ohtsu, H.; Nozaki, K.; Kitagawa, S.; Tanaka, K. *Inorg. Chem.* **2016**, *55* (5), 2076−2084.
(31) Sato, S.; Morikawa, T. *ChemPhotoChem.* **2018**, *2*, 207.
(32) Thompson, E. J.; Berben, L. A. *Angew. Chem., Int. Ed.* **2015**, *54* (40), 11642−11646.
(33) Qi, X.-J.; Fu, Y.; Liu, L.; Guo, Q.-X. *Organometallics* **2007**, *26* (17), 4197−4203.
(34) DuBois, D. L. *Inorg. Chem.* **2014**, *53* (8), 3935−3960.
(35) Bullock, R. M.; Appel, A. M.; Helm, M. L. *Chem. Commun.* **2014**, *50* (24), 3125−3143.
(36) Wiedner, E. S.; Chambers, M. B.; Pitman, C. L.; Bullock, R. M.; Miller, A. J.; Appel, A. M. *Chem. Rev.* **2016**, *116* (15), 8655−8692.
(37) Pitman, C. L.; Brereton, K. R.; Miller, A. J. *J. Am. Chem. Soc.* **2016**, *138* (7), 2252−2260.
(38) Brereton, K. R.; Bellows, S. M.; Fallah, H.; Lopez, A. A.; Adams, R. M.; Miller, A. J.; Jones, W. D.; Cundari, T. R. *J. Phys. Chem. B* **2016**, *120* (50), 12911−12919.
(39) Garg, K.; Matsubara, Y.; Ertem, M. Z.; Lewandowska-Andralojc, A.; Sato, S.; Szalda, D. J.; Muckerman, J. T.; Fujita, E. *Angew. Chem., Int. Ed.* **2015**, *54* (47), 14128−14132.
(40) Tsay, C.; Livesay, B. N.; Ruelas, S.; Yang, J. Y. *J. Am. Chem. Soc.* **2015**, *137* (44), 14114−14121.
(41) Taheri, A.; Berben, L. A. *Inorg. Chem.* **2016**, *55* (2), 378−385.
(42) Creutz, C.; Chou, M. H. *J. Am. Chem. Soc.* **2007**, *129* (33), 10108−10109.
(43) Wayner, D. D.; Parker, V. D. *Acc. Chem. Res.* **1993**, *26* (5), 287−294.
(44) Curtis, C. J.; Miedaner, A.; Ellis, W. W.; DuBois, D. L. *J. Am. Chem. Soc.* **2002**, *124* (9), 1918−1925.
(45) DuBois, D. L.; Berning, D. E. *Appl. Organomet. Chem.* **2000**, *14* (12), 860−862.
(46) Labinger, J. A.; Komadina, K. H. *J. Organomet. Chem.* **1978**, *155* (2), C25−C28.
(47) Curtis, C. J.; Miedaner, A.; Raebiger, J. W.; DuBois, D. L. *Organometallics* **2004**, *23* (3), 511−516.
(48) Nimlos, M. R.; Chang, C. H.; Curtis, C. J.; Miedaner, A.; Pilath, H. M.; DuBois, D. L. *Organometallics* **2008**, *27* (12), 2715−2722.
(49) Miedaner, A.; Haltiwanger, R. C.; DuBois, D. L. *Inorg. Chem.* **1991**, *30* (3), 417−427.
(50) Raebiger, J. W.; Miedaner, A.; Curtis, C. J.; Miller, S. M.; Anderson, O. P.; DuBois, D. L. *J. Am. Chem. Soc.* **2004**, *126* (17), 5502−5514.
(51) Berning, D. E.; Noll, B. C.; DuBois, D. L. *J. Am. Chem. Soc.* **1999**, *121* (49), 11432−11447.
(52) Berning, D. E.; Miedaner, A.; Curtis, C. J.; Noll, B. C.; Rakowski DuBois, M. C.; DuBois, D. L. *Organometallics* **2001**, *20* (9), 1832−1839.
(53) Wilson, A. D.; Miller, A. J.; DuBois, D. L.; Labinger, J. A.; Bercaw, J. E. *Inorg. Chem.* **2010**, *49* (8), 3918−3926.
(54) Ellis, W. W.; Ciancanelli, R.; Miller, S. M.; Raebiger, J. W.; Rakowski DuBois, M.; DuBois, D. L. *J. Am. Chem. Soc.* **2003**, *125* (40), 12230−12236.
(55) Roberts, J. A.; Appel, A. M.; DuBois, D. L.; Bullock, R. M. *J. Am. Chem. Soc.* **2011**, *133* (37), 14604−14613.
(56) Ellis, W. W.; Raebiger, J. W.; Curtis, C. J.; Bruno, J. W.; DuBois, D. L. *J. Am. Chem. Soc.* **2004**, *126* (9), 2738−2743.
(57) Ceballos, B. M.; Tsay, C.; Yang, J. Y. *Chem. Commun.* **2017**, *53* (53), 7405−7408.
(58) Creutz, C.; Chou, M. H. *J. Am. Chem. Soc.* **2009**, *131* (8), 2794−2795.
(59) Connelly, S. J.; Wiedner, E. S.; Appel, A. M. *Dalton Trans.* **2015**, *44* (13), 5933−5938.
(60) Taheri, A.; Thompson, E. J.; Fettinger, J. C.; Berben, L. A. *ACS Catal.* **2015**, *5* (12), 7140−7151.
(61) Connelly Robinson, S. J. C.; Zall, C. M.; Miller, D. L.; Linehan, J. C.; Appel, A. M. *Dalton Trans.* **2016**, *45* (24), 10017−10023.
(62) Waldie, K. M.; Ostericher, A. L.; Reineke, M.; Sasayama, A. F.; Kubiak, C. P. *ACS Catal.* **2018**, *8*, 1313.
(63) Cheng, J.; Handoo, K. L.; Parker, V. D. *J. Am. Chem. Soc.* **1993**, *115* (7), 2655−2660.
(64) Cheng, J.; Handoo, K. L.; Xue, J.; Parker, V. D. *J. Org. Chem.* **1993**, *58* (19), 5050−5054.
(65) Parker, V. *Acta Chem. Scand.* **1992**, *46* (11), 1133−1134.
(66) Zhu, X.-Q.; Wang, C.-H.; Liang, H.; Cheng, J.-P. *J. Org. Chem.* **2007**, *72* (3), 945−956.
(67) Zhang, X.-M.; Bruno, J. W.; Enyinnaya, E. *J. Org. Chem.* **1998**, *63* (14), 4671−4678.
(68) Handoo, K. L.; Cheng, J. P.; Parker, V. D. *J. Am. Chem. Soc.* **1993**, *115* (12), 5067−5072.
(69) Zhu, X.-Q.; Zhang, M.-T.; Yu, A.; Wang, C.-H.; Cheng, J.-P. *J. Am. Chem. Soc.* **2008**, *130* (8), 2501−2516.
(70) Han, X.; Hao, W.; Zhu, X.-Q.; Parker, V. D. *J. Org. Chem.* **2012**, *77* (15), 6520−6529.
(71) Zhu, X.-Q.; Tan, Y.; Cao, C.-T. *J. Phys. Chem. B* **2010**, *114* (5), 2058−2075.
(72) Richter, D.; Tan, Y.; Antipova, A.; Zhu, X. Q.; Mayr, H. *Chem. - Asian J.* **2009**, *4* (12), 1824−1829.
(73) Richter, D.; Mayr, H. *Angew. Chem., Int. Ed.* **2009**, *48* (11), 1958−1961.
(74) Hiromoto, T.; Warkentin, E.; Moll, J.; Ermler, U.; Shima, S. *Angew. Chem., Int. Ed.* **2009**, *48* (35), 6457−6460.
(75) Frisch, M. J.; Trucks, G. W.; Schlegel, H. B.; Scuseria, G. E.; Robb, M. A.; Cheeseman, J. R.; Scalmani, G.; Barone, V.; Mennucci, B.; Petersson, G. A.; Nakatsuji, H.; Caricato, M.; Li, X.; Hratchian, H. P.; Izmaylov, A. F.; Bloino, J.; Zheng, G.; Sonnenberg, J. L.; Hada, M.; Ehara, M.; Toyota, K.; Fukuda, R.; Hasegawa, J.; Ishida, M.; Nakajima, T.; Honda, Y.; Kitao, O.; Nakai, H.; Vreven, T.; Montgomery, J. A., Jr.; Peralta, J. E.; Ogliaro, F.; Bearpark, M.; Heyd, J. J.; Brothers, E.; Kudin, K. N.; Staroverov, V. N.; Kobayashi, R.; Normand, J.; Raghavachari, K.; Rendell, A.; Burant, J. C.; Iyengar, S. S.; Tomasi, J.; Cossi, M.; Rega, N.; Millam, J. M.; Klene, M.; Knox, J. E.; Cross, J. B.; Bakken, V.; Adamo, C.; Jaramillo, J.; Gomperts, R.; Stratmann, R. E.; Yazyev, O.; Austin, A. J.; Cammi, R.; Pomelli, C.; Ochterski, J. W.; Martin, R. L.; Morokuma, K.; Zakrzewski, V. G.; Voth, G. A.; Salvador, P.; Dannenberg, J. J.; Dapprich, S.; Daniels, A. D.; Farkas, O.;

DOI: 10.1021/jacs.7b13526
J. Am. Chem. Soc. 2018, 140, 4569−4579

Foresman, J. B.; Ortiz, J. V.; Cioslowski, J.; Fox, D. J. *Gaussian 09*, Revision A.02; Gaussian, Inc.: Wallingford, CT, 2009.
(76) Chai, J.-D.; Head-Gordon, M. *J. Chem. Phys.* **2008**, *128* (8), 084106.
(77) Chai, J.-D.; Head-Gordon, M. *Phys. Chem. Chem. Phys.* **2008**, *10* (44), 6615−6620.
(78) Barone, V.; Cossi, M. *J. Phys. Chem. A* **1998**, *102* (11), 1995−2001.
(79) Yang, X.; Walpita, J.; Zhou, D.; Luk, H. L.; Vyas, S.; Khnayzer, R. S.; Tiwari, S. C.; Diri, K.; Hadad, C. M.; Castellano, F. N.; et al. *J. Phys. Chem. B* **2013**, *117* (49), 15290−15296.
(80) Kelly, C. P.; Cramer, C. J.; Truhlar, D. G. *J. Phys. Chem. B* **2007**, *111* (2), 408−422.
(81) Muckerman, J. T.; Skone, J. H.; Ning, M.; Wasada-Tsutsui, Y. *Biochim. Biophys. Acta, Bioenerg.* **2013**, *1827* (8), 882−891.
(82) Lykke, K.; Murray, K.; Lineberger, W. *Phys. Rev. A: At., Mol., Opt. Phys.* **1991**, *43* (11), 6104.
(83) Becke, A. D. *J. Chem. Phys.* **1993**, *98* (7), 5648−5652.
(84) Grimme, S.; Ehrlich, S.; Goerigk, L. *J. Comput. Chem.* **2011**, *32* (7), 1456−1465.
(85) Weigend, F.; Ahlrichs, R. *Phys. Chem. Chem. Phys.* **2005**, *7* (18), 3297−3305.
(86) Marenich, A. V.; Cramer, C. J.; Truhlar, D. G. *J. Phys. Chem. B* **2009**, *113* (18), 6378−6396.
(87) Perdew, J. P. *Phys. Rev. B: Condens. Matter Mater. Phys.* **1986**, *33* (12), 8822.
(88) Neese, F. *Wiley Interdiscip Rev. Comput. Mol. Sci.* **2012**, *2* (1), 73−78.
(89) Isse, A. A.; Gennaro, A. *J. Phys. Chem. B* **2010**, *114* (23), 7894−7899.
(90) Ilic, S.; Brown, E. S.; Xie, Y.; Maldonado, S.; Glusac, K. D. *J. Phys. Chem. C* **2016**, *120* (6), 3145−3155.
(91) Laursen, B. W.; Krebs, F. C. *Chem. - Eur. J.* **2001**, *7* (8), 1773−1783.
(92) Paul, C. E.; Gargiulo, S.; Opperman, D. J.; Lavandera, I.; Gotor-Fernández, V.; Gotor, V.; Taglieber, A.; Arends, I. W.; Hollmann, F. *Org. Lett.* **2013**, *15* (1), 180−183.
(93) Huang, S.; Wong, J. C.; Leung, A. K.; Chan, Y. M.; Wong, L.; Fernendez, M. R.; Miller, A. K.; Wu, W. *Tetrahedron Lett.* **2009**, *50* (35), 5018−5020.
(94) Ogata, Y.; Takagi, K.; Tanabe, Y. *J. Chem. Soc., Perkin Trans. 2* **1979**, *8*, 1069−1071.
(95) Lee, C. K.; Lee, I.-S. H. *Heterocycles* **2009**, *78* (2), 425−433.
(96) Hori, M.; Kataoka, T.; Shimizu, H.; Imai, E.; Matsumoto, Y. *Chem. Pharm. Bull.* **1985**, *33* (9), 3681−3688.
(97) Carey, F. A.; Tremper, H. S. *J. Am. Chem. Soc.* **1968**, *90*, 2578−2583.
(98) Guin, J.; Besnard, C.; Pattison, P.; Lacour, J. *Chem. Sci.* **2011**, *2* (3), 425−428.
(99) Matthews, W. S.; Bares, J. E.; Bartmess, J. E.; Bordwell, F.; Cornforth, F. J.; Drucker, G. E.; Margolin, Z.; McCallum, R. J.; McCollum, G. J.; Vanier, N. R. *J. Am. Chem. Soc.* **1975**, *97* (24), 7006−7014.
(100) Connelly Robinson, S. J.; Zall, C. M.; Miller, D. L.; Linehan, J. C.; Appel, A. M. *Dalton Trans.* **2016**, *45* (24), 10017−10023.
(101) Cheng, J.-P.; Lu, Y.; Zhu, X.; Mu, L. *J. Org. Chem.* **1998**, *63* (18), 6108−6114.
(102) Pavlishchuk, V. V.; Addison, A. W. *Inorg. Chim. Acta* **2000**, *298* (1), 97−102.
(103) Shi, J.; Huang, X.-Y.; Wang, H.-J.; Fu, Y. *J. Chem. Inf. Model.* **2012**, *52* (1), 63−75.
(104) Muckerman, J. T.; Achord, P.; Creutz, C.; Polyansky, D. E.; Fujita, E. *Proc. Natl. Acad. Sci. U. S. A.* **2012**, *109* (39), 15657−15662.
(105) Kovács, G.; Pápai, I. *Organometallics* **2006**, *25* (4), 820−825.
(106) Keith, J. A.; Grice, K. A.; Kubiak, C. P.; Carter, E. A. *J. Am. Chem. Soc.* **2013**, *135* (42), 15823−15829.
(107) Bordwell, F. G. *Acc. Chem. Res.* **1988**, *21* (12), 456−463.
(108) Hapiot, P.; Moiroux, J.; Saveant, J. M. *J. Am. Chem. Soc.* **1990**, *112* (4), 1337−1343.
(109) Anne, A.; Hapiot, P.; Moiroux, J.; Savéant, J.-M. *J. Electroanal. Chem.* **1992**, *331* (1−2), 959−970.
(110) Hermolin, J.; Levin, M.; Kosower, E. M. *J. Am. Chem. Soc.* **1981**, *103* (16), 4808−4813.
(111) de Robillard, G.; Devillers, C. H.; Kunz, D.; Cattey, H.; Digard, E.; Andrieu, J. *Org. Lett.* **2013**, *15* (17), 4410−4413.
(112) Elangovan, A.; Chiu, H.-H.; Yang, S.-W.; Ho, T.-I. *Org. Biomol. Chem.* **2004**, *2* (21), 3113−3118.
(113) Gorodetsky, B.; Ramnial, T.; Branda, N. R.; Clyburne, J. A. *Chem. Commun.* **2004**, *17*, 1972−1973.
(114) Ogawa, K. A.; Boydston, A. J. *Chem. Lett.* **2014**, *43* (6), 907−909.
(115) Han, X.; Hao, W.; Zhu, X.-Q.; Parker, V. D. *J. Org. Chem.* **2012**, *77* (15), 6520−6529.
(116) Koper, N.; Jonker, S.; Verhoeven, J.; Van Dijk, C. *Recl. Trav. Chim. Pays-Bas* **1985**, *104* (11), 296−302.
(117) Heiden, Z. M.; Lathem, A. P. *Organometallics* **2015**, *34* (10), 1818−1827.
(118) Matsubara, Y.; Fujita, E.; Doherty, M. D.; Muckerman, J. T.; Creutz, C. *J. Am. Chem. Soc.* **2012**, *134* (38), 15743−15757.
(119) Kreevoy, M. M.; Ostovic, D.; Lee, I. S. H.; Binder, D. A.; King, G. W. *J. Am. Chem. Soc.* **1988**, *110* (2), 524−530.
(120) Brunet, P.; Wuest, J. D. *J. Org. Chem.* **1996**, *61* (6), 2020−2026.
(121) Shima, S.; Pilak, O.; Vogt, S.; Schick, M.; Stagni, M. S.; Meyer-Klaucke, W.; Warkentin, E.; Thauer, R. K.; Ermler, U. *Science* **2008**, *321* (5888), 572−575.
(122) McSkimming, A.; Colbran, S. B. *Chem. Soc. Rev.* **2013**, *42* (12), 5439−5488.
(123) Rakowski Dubois, M.; Dubois, D. L. *Acc. Chem. Res.* **2009**, *42* (12), 1974−1982.
(124) Thoi, V. S.; Sun, Y.; Long, J. R.; Chang, C. J. *Chem. Soc. Rev.* **2013**, *42* (6), 2388−2400.
(125) Miller, A. J.; Labinger, J. A.; Bercaw, J. E. *Organometallics* **2011**, *30* (16), 4308−4314.
(126) Pitman, C.; Finster, O.; Miller, A. *Chem. Commun.* **2016**, *52* (58), 9105−9108.
(127) Barrett, S. M.; Pitman, C. L.; Walden, A. G.; Miller, A. J. *J. Am. Chem. Soc.* **2014**, *136* (42), 14718−14721.
(128) Fraze, K.; Wilson, A. D.; Appel, A. M.; Rakowski DuBois, M.; DuBois, D. L. *Organometallics* **2007**, *26* (16), 3918−3924.
(129) Yang, J. Y.; Bullock, R. M.; Shaw, W. J.; Twamley, B.; Fraze, K.; DuBois, M. R.; DuBois, D. L. *J. Am. Chem. Soc.* **2009**, *131* (16), 5935−5945.
(130) Galan, B. R.; Schöffel, J.; Linehan, J. C.; Seu, C.; Appel, A. M.; Roberts, J. A.; Helm, M. L.; Kilgore, U. J.; Yang, J. Y.; DuBois, D. L.; Kubiak, C. P. *J. Am. Chem. Soc.* **2011**, *133* (32), 12767−12779.
(131) Yang, J. Y.; Smith, S. E.; Liu, T.; Dougherty, W. G.; Hoffert, W. A.; Kassel, W. S.; DuBois, M. R.; DuBois, D. L.; Bullock, R. M. *J. Am. Chem. Soc.* **2013**, *135* (26), 9700−9712.
(132) Carrillo, N.; Ceccarelli, E. A. *Eur. J. Biochem.* **2003**, *270* (9), 1900−1915.
(133) Evans, D. H. *Chem. Rev.* **2008**, *108* (7), 2113−2144.
(134) Evans, D. H.; Busch, R. W. *J. Am. Chem. Soc.* **1982**, *104* (19), 5057−5062.

DOI: 10.1021/jacs.7b13526
J. Am. Chem. Soc. 2018, 140, 4569−4579